

A hybrid origin for the Martian atmosphere

Kaveh Pahlevan^{1*}, Laura Schaefer², Don Porcelli³

1. Carl Sagan Center, SETI Institute, Mountain View, CA, USA
2. Department of Geological Sciences, Stanford University, Stanford, CA, USA
3. Department of Earth Sciences, Oxford University, Oxford, UK

*To whom correspondence should be addressed:

Email: kpahlevan@seti.org

Tel: +1 (480) 401 8584

2988 words abstract and captions included

30 references

4 Figures

Submitted to *Geochemical Perspectives Letters*

Keywords: Mars, primordial outgassing, atmosphere, nebular capture, hydrodynamic escape

1 **Abstract**

2 The Martian isotopic record displays a dichotomy in volatile compositions. Interior volatiles from
3 the mantle record a chondritic heritage (*e.g.*, H, N, Kr, Xe) whereas the atmospheric reservoir of
4 Kr and Xe – which do not currently experience escape – record heritage from a solar-like source.
5 Motivated by disparate inferences on the source of Martian atmospheric volatiles (outgassed
6 versus nebular captured), we consider hybrid-source accretionary atmospheres in which a high
7 molecular weight (*e.g.*, CO₂-rich) outgassed component is mixed in with the low molecular weight
8 H₂-He-rich nebular atmosphere. We conduct calculations of nebular capture with and without a
9 mixed-in high molecular weight outgassed component during the lifetime of the solar nebula.
10 Mixing in an outgassed component enhances the captured nebular inventory by ≈ 1 -3 orders of
11 magnitude – depending on the outgassed inventory – relative to “pure” nebular capture. These
12 observations and calculations suggest that the Martian atmosphere arose as a hybrid mixture of
13 outgassed and nebular-derived components and that – irrespective of the precise composition of
14 the outgassed component – was mainly composed of molecular hydrogen. The consequences for
15 Martian atmospheric history are discussed.

16

17 **1. Introduction**

18 Mars has recently emerged as a natural laboratory for studying the acquisition and processing of
19 volatile elements on the terrestrial planets. Because undifferentiated building blocks of terrestrial
20 planets were likely volatile-bearing (SCHAEFER AND FEGLEY, 2017) and Martian accretion likely
21 occurred in the presence of the volatile-rich solar nebula (DAUPHAS AND POURMAND, 2011),
22 questions about diverse volatile sources and formation processes for the primordial Martian
23 atmosphere can now be addressed (SAITO AND KURAMOTO, 2018; PÉRON AND MUKHOPADHYAY,

24 2022). High-precision isotopic measurements display a dichotomy in the sources of Martian
25 volatiles. Volatiles dissolved in melts derived from the Martian mantle are observed to have an
26 isotopic composition akin to chondrites for hydrogen, nitrogen, krypton and xenon (USUI, 2019;
27 PÉRON AND MUKHOPADHYAY, 2022; DELIGNY *et al.*, 2023) whereas the isotopic composition of
28 krypton and xenon in the Martian atmosphere – which do not currently experience escape – record
29 a solar-like source composition (PEPIN, 1991; CONRAD *et al.*, 2016). These observations prompt
30 questions about the relationship between Martian interior and atmospheric volatiles.

31

32 The volatile dichotomy between a chondrite-like mantle and a solar-like atmosphere has recently
33 been interpreted to mean that the Martian atmosphere cannot be the result of magma ocean
34 outgassing and must be the result of gravitational nebular capture (PÉRON AND MUKHOPADHYAY,
35 2022). There is, however, empirical isotopic evidence that silicate Mars experienced outgassing
36 during the lifetime of the short-lived and volatile radionuclide ^{129}I ($\tau_{1/2}=16$ Myrs), resulting in the
37 observed ^{129}Xe -depletion in Martian interior reservoirs (MARTY AND MARTI, 2002). Early selective
38 removal of volatile elements from silicate Mars – presumably via outgassing from a molten state
39 (ELKINS-TANTON, 2008) – points towards the transport of chondritic volatiles into the primordial
40 Martian atmosphere. Although this episode of primordial outgassing is empirically supported, it
41 has yet to be reconciled with the observed volatile dichotomy between the Martian interior and
42 atmosphere (PÉRON AND MUKHOPADHYAY, 2022). Here, we consider hybrid accretionary
43 atmospheres (SAITO AND KURAMOTO, 2018) in which an outgassed high-molecular weight gas is
44 mixed into the distended low-molecular weight nebular atmosphere. We show that such mixing
45 can reconcile primordial outgassing of chondritic volatiles with nebular capture of solar-like gases
46 into the Martian atmosphere, that mixing before dissipation of the solar nebula strongly enhances

47 the mass of nebular captured gas, and that comparison of hybrid-source compositions with that of
48 the present-day atmosphere can yield new insights into history of Martian atmospheric evolution.

49

50 **2. Results**

51 *Enhancement of nebular capture via mixing.* We calculate structures for captured Martian
52 atmospheres present during accretion in hydrostatic equilibrium and thermal steady state with the
53 solar nebula. We consider atmospheres both with and without mixing of an outgassed high mean
54 molecular weight layer (see Supplementary Information for a discussion on mixing). Atmospheres
55 without a high molecular weight component are called “pure” and are presented as a reference.
56 The atmospheres are convective at depth and radiative at altitude, and are assumed to blend into
57 the solar nebula at the Hill radius at ≈ 320 Mars radii. Because the mass (and heat capacity) of these
58 atmospheres is relatively small, a heat source other than secular cooling is needed to calculate
59 quasi-static structures. An absolute lower limit on the heat flow derives from long-lived radioactive
60 decay and is equivalent to accretion rates $\approx 10^{-4}$ Mars masses/Myr (ERKAEV *et al.*, 2014). More
61 likely heat flows relevant to the first few million years of Martian history derive from ongoing
62 planetesimal accretion and/or ^{26}Al decay. We consider heat flows at the base of the atmosphere
63 equivalent to planetesimal accretion rates of 0.01-1 Mars masses/Myr, covering the range from
64 energetic accretion consistent with large-scale melting (DAUPHAS AND POURMAND, 2011) down to
65 reduced heat flows unable to maintain a magma ocean (SAITO AND KURAMOTO, 2018) and more
66 consistent with sweep-up of planetesimals during the waning stages of accretion. For heat flows
67 equivalent to accretion rates of 0.01-1 Mars masses/Myr, the mass (M_{H}) of a “pure” nebular
68 captured atmosphere is $\approx 0.2\text{-}3.1 \times 10^{18}$ kg and equivalent to $\approx 0.05\text{-}0.8$ bars of H_2 at the Mars surface

69 (Fig. 1). Lower accretion rates produce cooler, denser atmospheres that are also more massive, a
70 behaviour summarized with the maxim: “to cool is to accrete” (LEE AND CHIANG, 2015).

71

72 Mixing of the nebular atmosphere with an outgassed high molecular weight gas sharply enhances
73 the mass of the captured gas inventory. To illustrate the magnitude of this effect, we calculate the
74 structure of hybrid-source atmospheres in which the outgassed component consists of pure CO₂
75 ($\mu=44$ amu with an inventory size characterized by M_{CO_2}) with the nebular component ($\mu=2.4$ amu
76 with an inventory size characterized by M_{H}) assumed to be fully-mixed into the outgassed layer,
77 producing a homogeneous hybrid-source atmosphere (see Supplementary Information for details).

78 When this well-mixed atmosphere hydrostatically equilibrates with the solar nebula and achieves
79 thermal steady state, the mass of the captured inventory (M_{H}) strongly depends on the inventory
80 of the high molecular weight gas (M_{CO_2}) with which it is mixed (see Gas-assisted capture, Fig. 1).

81 For planetesimal accretion rates of 0.01-1 Mars masses/Myr and heavy gas inventories ($M_{\text{CO}_2}=3.9-$
82 390×10^{19} kg) equivalent to 10-1000 bars of CO₂ at the planetary surface (ELKINS-TANTON, 2008),
83 the captured nebular inventory (M_{H}) is in the range of $1.2-120 \times 10^{19}$ kg, equivalent to $\approx 3-300$ bars
84 of H₂ at the surface (Fig. 1). The strong enhancement of nebular gravitational capture via mixing

85 an outgassed component can be understood by considering the increase in mean molecular weight,
86 which increases the gravitational coupling between the atmosphere and planet and decreases the

87 atmospheric scale height, which – like cooling – causes contraction and an increase in the hydrogen
88 density of the lower atmosphere where most of the atmospheric mass resides. This behaviour can

89 be summarized with another maxim: “to mix is to accrete.”

90

91 The dependence of the nebular captured inventory (M_H) on the outgassed inventory (M_{CO_2}) in
92 fully-mixed hybrid-source atmospheres (Fig. 1) sets upper limits on the contribution of the nebular
93 component to the Martian atmosphere. A measure of the relative contribution of captured and
94 outgassed inventories is the mean molecular weight of the mixture, which is constant to within a
95 factor of \sim three for the full range of conditions we calculate ($\mu=6.6-19$ amu) (Fig. 1). Although
96 most of the mass of the outgassed component is dominated by carbon species (*e.g.*, CO_2), other
97 outgassed volatiles (H, N, and noble gases) were also present and the elemental abundances and
98 isotopic composition of the hybrid mixture can be used – in comparison with observed abundances
99 – to further constrain the nebular contribution to Martian volatiles. Whereas the physics of nebular
100 capture into fully-mixed hybrid atmospheres yields upper limits on the nebular contribution, lower
101 limits can be derived from the cosmochemistry of chondritic-nebular gas mixtures, as we show in
102 the following section.

103

104 ***Chondritic-nebular gas mixtures.*** To describe cosmochemical consequences of mixing a nebular
105 component into an outgassed atmosphere, we calculate two-component mixtures including major
106 volatiles (H, C, N) and noble gases (Ar, Kr, Xe) with chondritic and nebular endmembers. We
107 neglect He and Ne because – like He in Earth’s atmosphere – the lifetime of these noble gases with
108 respect to escape from the Martian atmosphere is thought to be short relative to geological
109 timescales and their present-day abundances may simply reflect a balance between recent supply
110 and loss (KUROKAWA *et al.*, 2021). For the chondritic endmember, we adopt the 55% H chondrite
111 45% EH chondrite model for Mars (SANLOUP *et al.*, 1999). For the purposes of the mixing
112 calculations, we include all chondritic volatiles (interior and outgassed), although a substantial
113 fraction of chondritic H (or “water”) is expected to remain sequestered in the interior (SIM *et al.*,

114 2024). The assumption of complete outgassing may be more accurate in the case of C, N, and the
115 noble gases. With endmember compositions specified, the composition of the resulting mixture
116 can be described with one parameter, the relative contribution of the two components.

117

118 The compositional characteristics of a nebular-chondritic mixture can be calculated for comparison
119 with the observed atmospheric abundances. For “Gas assisted capture” (Fig. 1), representing fully-
120 mixed hybrid-sourced atmospheres in hydrostatic equilibrium with the solar nebula, the nebular
121 contribution to the total volatile budget of Mars, counting atoms, is $\approx 46\text{-}77\%$, depending on the
122 accretion rate and outgassed volatile inventory. The total volatile budget is dominated by H and
123 He from the nebular component and H and C from the chondritic component. For these relative
124 proportions of the nebular component to the hybrid mixture, the argon ($>99\%$) and krypton ($>90\%$)
125 inventories are dominated by the nebular component, whereas carbon ($<1\%$) and nitrogen ($<2\%$)
126 inventories experience negligible nebular additions and continue to be dominated by the outgassed
127 component (Fig. 2). Hydrogen and xenon are intermediate cases in which the inventories in the
128 resulting mixture are derived from comparable contributions from the two sources. In summary,
129 nebular capture via complete mixing into a hybrid-source atmosphere produces Martian Ar and Kr
130 with solar heritage, C and N with chondritic heritage, and H and Xe with mixed heritage.

131

132 A hybrid primordial mixture is consistent with the observed isotopic composition of the Martian
133 atmosphere. Mass-selective loss has fractionated stable Ar isotopes (^{36}Ar from ^{38}Ar) but a solar-
134 like source is a viable starting composition for atmospheric argon (ATREYA *et al.*, 2013). Krypton
135 in the atmosphere is isotopically distinct from chondrites but indistinguishable from solar (PEPIN,
136 1991). Atmospheric xenon can be modelled as either mass-fractionated solar or mass-fractionated

137 chondritic gas (SWINDLE, 2002). Although the physics of nebular capture into fully-mixed hybrid
138 atmospheres sets upper limits on the nebular contribution (<46-77%), partial mixing could yield a
139 lower nebular contribution. The requirement that Martian Kr be indistinguishable from solar but
140 distinct from chondrites conservatively constrains the nebular contribution to the total Martian
141 volatile budget to >10%, counting atoms (Fig. 2). Next, we consider the consequences of
142 primordial hybrid mixtures for inferring Martian atmospheric history.

143

144 ***Elemental abundances elucidate escape processes.*** Of all the major volatiles (H, C, N) and noble
145 gases (Ar, Kr, Xe) we consider, krypton alone is isotopically unfractionated in Mars's atmosphere
146 relative to its apparent source, the solar nebula. Accordingly, to gain insight into the nature of
147 evolutionary processes, we consider elemental abundances normalized to krypton and relative to
148 solar composition. Hybrid-source elemental abundances have some affinity to modern Mars (Fig.
149 3), with important differences. Relative to hybrid-source mixtures, the modern Martian atmosphere
150 is elementally depleted in H, C, N, Ar, and Xe, each of which is also enriched in heavy isotopes in
151 the Martian atmosphere (BOGARD *et al.*, 2001). Such coupled elemental and isotopic fractionation
152 suggests the viability of a hybrid-source mixture as a precursor to the modern Martian atmosphere,
153 the two being linked via compositional evolutionary processes, among which mass-selective losses
154 to space looms large.

155

156 We consider elemental ($^{36}\text{Ar}/^{84}\text{Kr}$) and stable isotopic ($^{36}\text{Ar}/^{38}\text{Ar}$) fractionation accompanying
157 argon loss. Argon is suitable for examining ancient processes because the inventory of atmospheric
158 ^{36}Ar is primordial meaning it cannot be accounted for by volcanic outgassing over time (JAKOSKY
159 AND TREIMAN, 2023). The non-radiogenic Ar/Kr ratio in the modern Martian atmosphere is lower

160 than that of a hybrid mixture by a factor of ≈ 50 (Fig. 3) whereas the $^{36}\text{Ar}/^{38}\text{Ar}$ is only lower than
161 plausible sources by $\approx 25\%$ (ATREYA *et al.*, 2013). A loss process that strongly separates Ar from
162 Kr but only weakly discriminates ^{36}Ar from ^{38}Ar is indicated. We consider an episode of extreme
163 ultraviolet (EUV) powered hydrodynamic escape in which an outflow of H_2 and CO_2 entrains trace
164 gases via frequent collisions (ZAHNLE *et al.*, 1990). This is thought to be the main loss process by
165 which H_2 -dominated atmospheres dissipate (LAMMER *et al.*, 2014). Entrainment involves all trace
166 gases up to a maximum molecular mass whose value depends on the strength of the escape flow
167 (See Supplementary Information for details). Model results reveal the existence of a hydrodynamic
168 outflow sufficiently strong to reproduce the chemical (Ar/Kr) and isotopic ($^{36}\text{Ar}/^{38}\text{Ar}$) fractionation
169 observed in the Martian atmosphere starting from a hybrid mixture while remaining sufficiently
170 weak to allow Kr to be retained and its solar isotopic heritage to be preserved (Fig. 4). Of course,
171 mass-selective argon loss from Mars via other mechanisms (*e.g.*, solar wind sputtering) occurs and
172 is ongoing (JAKOSKY *et al.*, 2017). The hybrid mixture model provides a framework for assessing
173 the relative importance of various mechanisms of Martian atmospheric loss over the entire history
174 of the planet.

175

176 **3. Discussion**

177 ***The origin of the Martian hydrosphere.*** A significant feature of the Martian volatile record is that
178 the surface hydrosphere inferred by geomorphology – like the atmospheric ^{36}Ar reservoir – cannot
179 be generated via volcanic outgassing over time (JAKOSKY AND TREIMAN, 2023). The hydrosphere
180 was apparently placed on the Martian surface early in planetary history. Independent evidence for
181 the existence of a Martian surface hydrosphere in the first 100 Myrs comes from an excess of ^{129}Xe
182 in the atmosphere from the decay of water-soluble and short-lived ^{129}I (MUSSELWHITE *et al.*, 1991).

183 The hybrid origin model for the Martian atmosphere suggests a new mechanism for the formation
184 of a hydrosphere. Although we have considered the nebular and chondritic gases to be chemically
185 inert, in reality, the H₂-dominated nebular gas can react with outgassed oxides (e.g., CO₂) to
186 produce new planetary water (H₂+CO₂→H₂O+CO). If the CO thus produced escapes as CO, there
187 is a net gain of water at the Martian surface. Both the strong D/H enrichment of the early Martian
188 hydrosphere (GREENWOOD *et al.*, 2008) and the anomalous oxygen recorded in ~4.43 billion year
189 old zircons (NEMCHIN *et al.*, 2014) may result from isotopic exchange between a hydrosphere and
190 an escaping H₂-dominated atmosphere (PAHLEVAN *et al.*, 2022; ZAHNLE AND KASTING, 2023).

191

192 ***Cometary contribution to the inner Solar System.*** The low C/³⁶Ar and N/³⁶Ar of the Martian
193 atmosphere relative to chondrites (Fig. 3) has previously been attributed to a possible contribution
194 from comets, which are expected to be Ar-rich (MARTY *et al.*, 2016). However, a cometary origin
195 introduces some problems even as it solves others. Results from the Rosetta mission allowed the
196 identification of cometary xenon as a likely source for terrestrial atmospheric xenon, in particular
197 the long-hypothesized component called U-Xe that is apparent in the atmosphere of Earth but not
198 Mars (MARTY *et al.*, 2017). Assuming comet 67P/Churyumov-Gerasimenko – which Rosetta
199 sampled – is representative of the cometary reservoir, the question arises as to why the Martian
200 atmospheric xenon does not record any signature of a cometary component. The resolution to this
201 dilemma may be the relative retention of volatiles during impacts onto Earth and Mars. Cometary
202 impacts onto terrestrial planets are high-velocity events sufficiently energetic to vaporize both icy
203 and silicate components, producing impact vapor plumes. The fate of impact plumes (retained or
204 lost) depends on the ratio of impact to escape velocity, such that cometary vapor plumes on Earth
205 tend to be gravitationally retained whereas those on Mars tend to disperse from the weaker gravity

206 field present (ZAHNLE, 1993). More work is needed to better understand the role of various escape
207 processes in sculpting the volatile inventory of the terrestrial planets.

208

209 **Acknowledgements**

210 K.P. acknowledges support from NASA's Solar System Workings Program (80NSSC21K1833).

211 The authors acknowledge discussions with Sujoy Mukhopadhyay and comments on an early draft

212 from Kevin Zahnle, Alessandro Morbidelli, and James Lyons, which helped to improve the

213 manuscript.

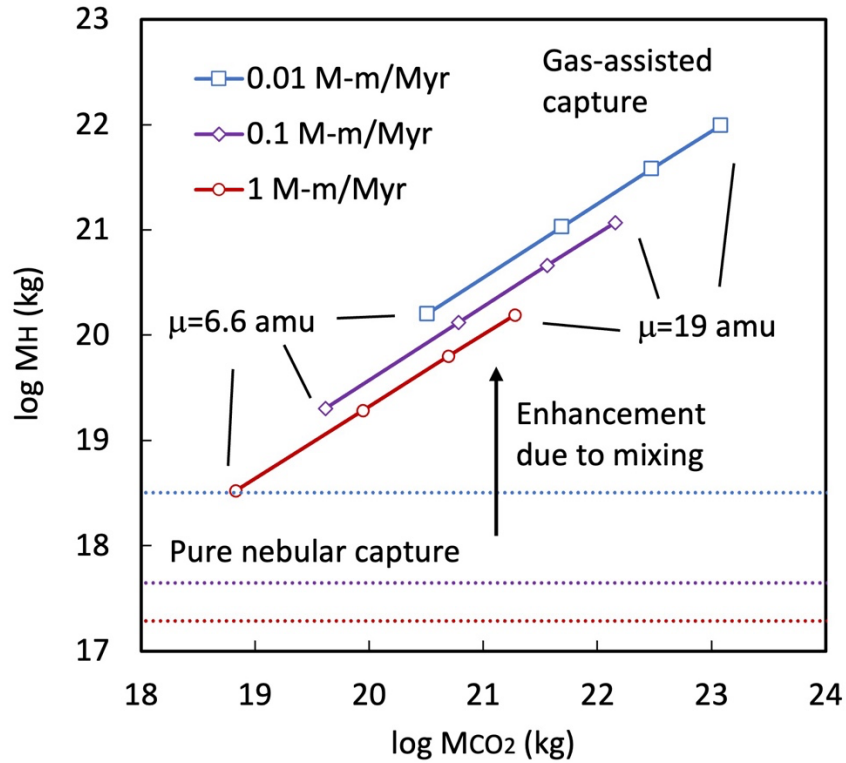


Figure 1. The captured gas inventory (M_H) as a function of the outgassed inventory (M_{CO_2}) for fully-mixed hybrid atmospheres. Curves correspond to different accretion rates (in units of Mars masses per million years) and therefore to different planetary luminosities. “Pure nebular capture” (dotted lines) refer to nebular atmospheres with no outgassed component mixed in ($M_{CO_2}=0$) for reference. Mixing with a high molecular weight component promotes nebular capture with the magnitude of the enhancement dependent on the mixed in heavy gas inventory.

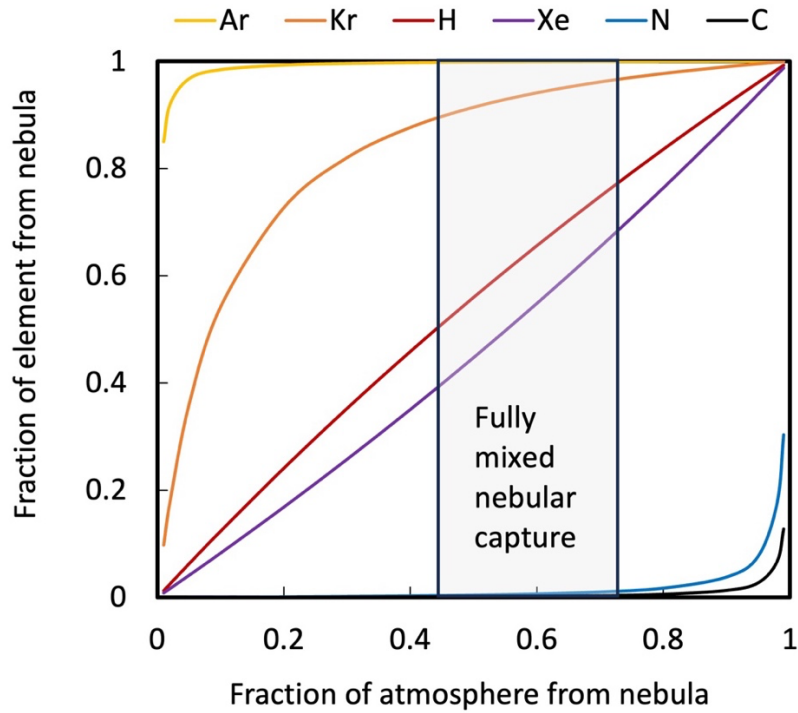


Figure 2. Mixtures of chondritic and solar-composition gases make specific predictions for the provenance of elements deriving from each component. The krypton isotopic composition of the Martian atmosphere – like solar and distinct from chondrites (PEPIN, 1991) – suggests the nebular contribution to the primordial Martian atmosphere was >10% counting atoms. Upper limits on the contribution of the nebular component to Martian volatiles derive from the physics of nebular capture into fully mixed hybrid atmospheres and are <46-77% (see Fig. 1).

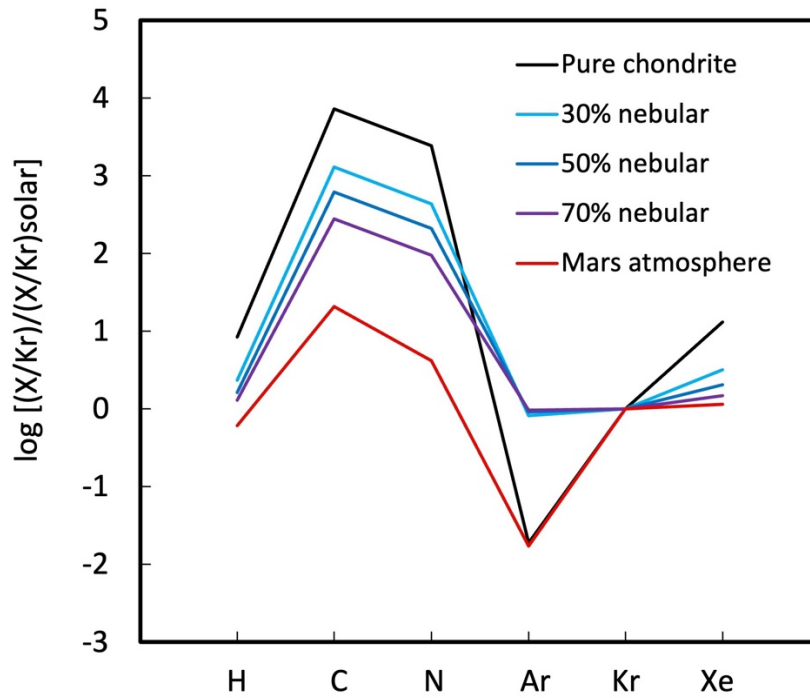


Figure 3. Relative abundances of volatile elements in mixtures of chondritic and solar composition gases normalized to krypton and to solar composition. Percentages refer to the fraction of total atoms in the mixture contributed by the solar component. Mixtures with varying proportions of the nebular component can be compared to the composition of the present-day Martian atmosphere and differences between the two compositions used to infer the imprints of loss processes.

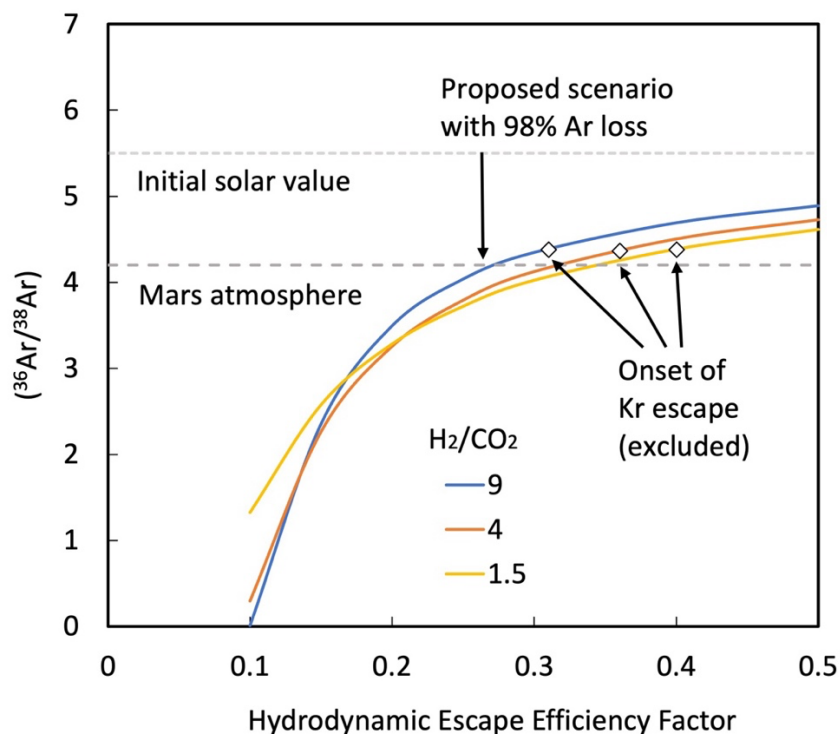


Figure 4. Mass-dependent fractionation accompanying argon loss from the hybrid Mars atmosphere. The solid lines show the argon isotopic composition of an atmosphere after mass-fractionation via Rayleigh distillation driven by hydrodynamic escape, for various hybrid nebular and chondritic proportions (H_2/CO_2), starting with solar Ar ($^{36}Ar/^{38}Ar=5.5$). The efficiency factor is a proxy for the mass-loss rate. Preservation of the solar isotopic Kr requires Kr non-participation in the mass-fractionating outflow and sets upper limits on the efficiency factor. The existence of solutions sufficiently vigorous to allow large (50x) reductions in Ar/Kr (see Fig. 3) without excessive Ar (and no Kr) isotopic fractionation indicates the viability of a hybrid mixture as the initial composition of the Martian atmosphere.

References

- 214 Atreya, S.K., Trainer, M.G., Franz, H.B., Wong, M.H., Manning, H.L., Malespin, C.A., Mahaffy, P.R.,
215 Conrad, P.G., Brunner, A.E., Leshin, L.A. (2013) Primordial argon isotope fractionation in
216 the atmosphere of Mars measured by the SAM instrument on Curiosity and implications
217 for atmospheric loss. *Geophysical Research Letters* 40, 5605-5609.
- 218 Bogard, D., Clayton, R., Marti, K., Owen, T., Turner, G. (2001) Martian volatiles: Isotopic
219 composition, origin, and evolution *Chronology and Evolution of Mars: Proceedings of an*
220 *ISSI Workshop, 10–14 April 2000, Bern, Switzerland*. Springer.
- 221 Conrad, P.G., Malespin, C.A., Franz, H.B., Pepin, R.O., Trainer, M.G., Schwenzer, S.P., Atreya, S.,
222 Freissinet, C., Jones, J., Manning, H. (2016) In situ measurement of atmospheric krypton
223 and xenon on Mars with Mars Science Laboratory. *Earth and Planetary Science Letters*
224 454, 1-9.
- 225 Dauphas, N., Pourmand, A. (2011) Hf-W-Th evidence for rapid growth of Mars and its status as a
226 planetary embryo. *Nature* 473, 489-U227.
- 227 Deligny, C., Füre, E., Deloule, E., Peslier, A., Faure, F., Marrocchi, Y. (2023) Origin of nitrogen on
228 Mars: First in situ N isotope analyses of martian meteorites. *Geochimica et Cosmochimica*
229 *Acta* 344, 134-145.
- 230 Elkins-Tanton, L.T. (2008) Linked magma ocean solidification and atmospheric growth for Earth
231 and Mars. *Earth and Planetary Science Letters* 271, 181-191.
- 232 Erkaev, N., Lammer, H., Elkins-Tanton, L., Stökl, A., Odert, P., Marcq, E., Dorfi, E., Kislyakova, K.,
233 Kulikov, Y.N., Leitzinger, M. (2014) Escape of the martian protoatmosphere and initial
234 water inventory. *Planetary and Space Science* 98, 106-119.
- 235 Greenwood, J.P., Itoh, S., Sakamoto, N., Vicenzi, E.P., Yurimoto, H. (2008) Hydrogen isotope
236 evidence for loss of water from Mars through time. *Geophysical Research Letters* 35.
- 237 Jakosky, B.M., Slipski, M., Benna, M., Mahaffy, P., Elrod, M., Yelle, R., Stone, S., Alsaeed, N. (2017)
238 Mars' atmospheric history derived from upper-atmosphere measurements of $^{38}\text{Ar}/^{36}\text{Ar}$.
239 *Science* 355, 1408-1410.
- 240 Jakosky, B.M., Treiman, A.H. (2023) Mars volatile inventory and outgassing history. *Icarus* 402,
241 115627.
- 242 Kurokawa, H., Miura, Y.N., Sugita, S., Cho, Y., Leblanc, F., Terada, N., Nakagawa, H. (2021) Mars'
243 atmospheric neon suggests volatile-rich primitive mantle. *Icarus* 370, 114685.
- 244 Lammer, H., Stökl, A., Erkaev, N., Dorfi, E., Odert, P., Güdel, M., Kulikov, Y.N., Kislyakova, K.,
245 Leitzinger, M. (2014) Origin and loss of nebula-captured hydrogen envelopes from 'sub'-
246 to 'super-Earths' in the habitable zone of Sun-like stars. *Monthly Notices of the Royal*
247 *Astronomical Society* 439, 3225-3238.
- 248 Lee, E.J., Chiang, E. (2015) To cool is to accrete: analytic scalings for nebular accretion of planetary
249 atmospheres. *The Astrophysical Journal* 811, 41.
- 250 Marty, B., Altwegg, K., Balsiger, H., Bar-Nun, A., Bekaert, D.V., Berthelier, J.-J., Bieler, A., Briois,
251 C., Calmonte, U., Combi, M., De Keyser, J., Fiethe, B., Fuselier, S.A., Gasc, S., Gombosi, T.I.,
252 Hansen, K.C., Hässig, M., Jäckel, A., Kopp, E., Korth, A., Le Roy, L., Mall, U., Mousis, O.,
253 Owen, T., Rème, H., Rubin, M., Sémon, T., Tzou, C.-Y., Waite, J.H., Wurz, P. (2017) Xenon
254 isotopes in 67P/Churyumov-Gerasimenko show that comets contributed to Earth's
255 atmosphere. *Science* 356, 1069-1072.

256 Marty, B., Avice, G., Sano, Y., Altwegg, K., Balsiger, H., Hässig, M., Morbidelli, A., Mousis, O.,
257 Rubin, M. (2016) Origins of volatile elements (H, C, N, noble gases) on Earth and Mars in
258 light of recent results from the ROSETTA cometary mission. *Earth and Planetary Science*
259 *Letters* 441, 91-102.

260 Marty, B., Marti, K. (2002) Signatures of early differentiation of Mars. *Earth and Planetary Science*
261 *Letters* 196, 251-263.

262 Musselwhite, D.S., Drake, M.J., Swindle, T.D. (1991) Early outgassing of Mars supported by
263 differential water solubility of iodine and xenon. *Nature* 352, 697-699.

264 Nemchin, A., Humayun, M., Whitehouse, M., Hewins, R., Lorand, J., Kennedy, A., Grange, M.,
265 Zanda, B., Fieni, C., Deldicque, D. (2014) Record of the ancient martian hydrosphere and
266 atmosphere preserved in zircon from a martian meteorite. *Nature Geoscience* 7, 638-642.

267 Pahlevan, K., Schaefer, L., Elkins-Tanton, L.T., Desch, S.J., Buseck, P.R. (2022) A primordial
268 atmospheric origin of hydrospheric deuterium enrichment on Mars. *Earth and Planetary*
269 *Science Letters* 595, 117772.

270 Pepin, R.O. (1991) On the origin and early evolution of terrestrial planet atmospheres and
271 meteoritic volatiles. *Icarus* 92, 2-79.

272 Péron, S., Mukhopadhyay, S. (2022) Krypton in the Chassigny meteorite shows Mars accreted
273 chondritic volatiles before nebular gases. *Science* 377, 320-324.

274 Saito, H., Kuramoto, K. (2018) Formation of a hybrid-type proto-atmosphere on Mars accreting
275 in the solar nebula. *Monthly Notices of the Royal Astronomical Society* 475, 1274-1287.

276 Sanloup, C., Jambon, A., Gillet, P. (1999) A simple chondritic model of Mars. *Physics of the Earth*
277 *and Planetary Interiors* 112, 43-54.

278 Schaefer, L., Fegley, B. (2017) Redox States of Initial Atmospheres Outgassed on Rocky Planets
279 and Planetesimals. *The Astrophysical Journal* 843, 120.

280 Sim, S.J., Hirschmann, M.M., Hier-Majumder, S. (2024) Volatile and trace element storage in a
281 crystallizing martian magma ocean. *Journal of Geophysical Research: Planets* 129,
282 e2024JE008346.

283 Swindle, T.D. (2002) Martian noble gases. *Reviews in Mineralogy and Geochemistry* 47, 171-190.

284 Usui, T. (2019) Hydrogen reservoirs in Mars as revealed by martian meteorites, *Volatiles in the*
285 *Martian Crust*. Elsevier, 71-88.

286 Zahnle, K., Kasting, J.F., Pollack, J.B. (1990) Mass fractionation of noble gases in diffusion-limited
287 hydrodynamic hydrogen escape. *Icarus* 84, 502-527.

288 Zahnle, K.J. (1993) Xenological constraints on the impact erosion of the early Martian
289 atmosphere. *Journal of Geophysical Research: Planets* 98, 10899-10913.

290 Zahnle, K.J., Kasting, J.F. (2023) Elemental and isotopic fractionation as fossils of water escape
291 from Venus. *Geochimica et Cosmochimica Acta* 361, 228-244.

A hybrid origin for the Martian atmosphere

K. Pahlevan, L. Schaefer, D. Porcelli

Supplementary Information

The Supplementary Information includes:

- Enhancement of Nebular Capture
- Energetics and Mechanism of Fluid Mixing
- Fractionation via Hydrodynamic Escape
- Supplementary Tables S-1 and S-2
- Supplementary Information References

Enhancement of Nebular Capture

Pure nebular captured atmospheres

The structure of a planetary atmosphere in hydrostatic equilibrium and thermal steady state with a gas disk is related to the planetary luminosity and the temperature (T_H) and density (ρ_H) of the gas disk in which it is embedded (HAYASHI *et al.*, 1979). For nebular conditions at the radial distance of Mars, we adopt $T_H = 200\text{ K}$ and $\rho_H = 5 \cdot 10^{-10}\text{ g cm}^{-3}$ (HAYASHI, 1981). We take the outer boundary of the atmosphere where the hydrostatic structure continuously connects to the solar nebula as the Hill radius, $R_H[\equiv a \cdot (M_p/3M_*)^{1/3}]$, with a the semi-major axis of the planetary orbit, M_p the planetary mass, and M_* the stellar mass. R_H for Mars is ≈ 320 planetary radii. We note that different model assumptions are possible (e.g., outer boundary at $R_H/4$) (CHAMBERS, 2017) but that choice of outer boundary condition has only a minor effect on calculated densities lower in the atmosphere where most of the mass resides (PISO AND YODIN, 2014).

The mass of the nebular-captured atmosphere is calculated using the minimum of the Hill radius and the Bondi radius $R_B[\equiv GM_p\bar{\mu}/k_B T_H]$ (IKOMA AND GENDA, 2006) with G is the universal gravitational constant, $\bar{\mu}$ the mean molecular weight of the atmosphere ($=2.4$ amu for a H_2 -He-rich nebular gas), and k_B Boltzmann's constant. For nebular capture onto Mars, the Bondi radius is smaller than the Hill radius by about an order of magnitude. Hence, even though the Hill sphere is the outer boundary where hydrostatic equilibrium with the solar nebula is assumed, captured atmospheric masses are calculated by considering only the mass inside the Bondi radius.

To calculate vertical temperature and density structure, we consider compositionally uniform two-layer atmospheres in which the lower layer is convective and the upper layer is radiative. At the bottom of the atmosphere, we consider heat input via gravitational energy release due to planetesimal accretion:

$$L_{in} = \frac{GM_p\dot{M}_p}{R_p} \quad (\text{Eq. S-1})$$

with M_p and R_p the planetary mass and radius, and \dot{M}_p the mass accretion rate, which we take to be 0.01-1 Mars mass/Myr. ^{26}Al heating may also be relevant for early Mars but can be modelled using this range of accretion rates. In

quasi-steady state, this heat input is balanced by radiative heat losses at the radiative-convective boundary of the surrounding atmosphere (GINZBURG *et al.*, 2016):

$$L_{out} = \frac{64\pi\sigma_{SB}T_{rcb}^4 R'_B}{3\kappa_{rcb}\rho_{rcb}} \quad (\text{Eq. S-2})$$

with σ_{SB} the Stefan-Boltzmann constant, T_{rcb} the temperature at the radiative-convective boundary, which is the same as the nebular temperature to within a factor of order unity (PISO AND YODIN, 2014), κ_{rcb} and ρ_{rcb} are the opacity and density at the radiative-convective boundary, and R'_B is the modified Bondi radius:

$$R'_B = \frac{\gamma-1}{\gamma} \frac{GM_p\bar{\mu}}{k_B T_H} \quad (\text{Eq. S-3})$$

with γ the adiabatic index, for which we adopt a value appropriate for diatomic molecules (7/5) (KITTEL AND KROEMER, 1998). For our analysis, we make the approximation that $T_{rcb} = T_H$. To solve for the atmospheric structure, a prescription for the opacity is needed. We assume atmospheric opacity is dominated by dust with a size-distribution like that of the interstellar medium (BELL AND LIN, 1994):

$$\kappa = 2 \cdot \left(\frac{T}{100 \text{ K}}\right)^2 \text{ cm}^2 \text{ g}^{-1} \quad (\text{Eq. S-4})$$

With these equations, it is possible to solve for the density at the radiative-convective boundary (ρ_{rcb}) as a function of the planetesimal accretion rate (\dot{M}_p), which is one of the parameters that determines the total mass of captured gas. In addition, we solve for the radial distance of the radiative-convective boundary (R_{rcb}). Approximating the radiative layer above the radiative-convective boundary as an isothermal layer in hydrostatic equilibrium to the Hill sphere, we obtain:

$$\frac{R_{rcb}}{R_B} = \left[\ln\left(\frac{\rho_{rcb}}{\rho_H}\right) + \frac{R_B}{R_H} \right]^{-1} \quad (\text{Eq. S-5})$$

With these parameters, we solve for the radius of the radiative-convective boundary (R_{rcb}) as a function of the density at that location (ρ_{rcb}). Because atmospheric mass in the radiative layer is negligible due to the exponentially decreasing density in that region (PISO AND YODIN, 2014), the total mass of the nebular captured atmosphere can be expressed by integrating the density structure of the lower adiabatic convective layer (GINZBURG *et al.*, 2016):

$$M_H = \left(\frac{5\pi^2}{4}\right) R_{rcb}^3 \rho_{rcb} \left(\frac{R'_B}{R_{rcb}}\right)^{\frac{1}{\gamma-1}} \quad (\text{Eq. S-6})$$

Fully-mixed hybrid atmospheres

A fully-mixed hybrid atmosphere is one in which the outgassed components (e.g., CO₂) and the nebular captured gases are present in uniform proportions throughout the Hill sphere. A fully-mixed state describes the maximum enhancement of the nebular captured gaseous inventory and is therefore a useful and easily calculable state. Identical expressions for the incoming luminosity (L_{in}), outgoing luminosity (L_{out}), and modified Bondi sphere (R'_B) (Eq. S-1, S-2, and S-3) can be used. An important difference is that the mean molecular weight within the Hill sphere is no longer equal to that of the surrounding nebular environment but is given by the proportion of outgassed and nebular captured components:

$$\bar{\mu} = x_H \mu_H + (1 - x_H) \mu_{CO_2} \quad (\text{Eq. S-7})$$

where x_H represents the mole fraction of gas species that derive from the nebular component, with μ_H and μ_{CO_2} equal 2.4 and 44 amu, respectively. Two other adjustments to the capture model must be made to accommodate uniform mixing with an outgassed heavy gas component. First, the opacity law we have adopted (Eq. S-4) is appropriate to dust-dominated opacity, which may be the case for the nebular captured component but not the outgassed component, which is thought to be exsolved from a magma ocean and is assumed to be dust-free. Accordingly, we assume that the opacity of the mixture is dominated by the opacity of dust in the nebular component, and adopt an expression for a lower opacity relative to a pure nebular atmosphere:

$$\kappa = 2 \cdot \left(\frac{T}{100 \text{ K}}\right)^2 \cdot x_H \cdot \left(\frac{\mu_H}{\bar{\mu}}\right) \text{ cm}^2 \text{ g}^{-1} \quad (\text{Eq. S-8})$$

The procedure for calculating fully-mixed hybrid atmosphere solutions is to take the mole fraction of the nebular component (x_H) as an independent variable and select a value, which in practice is in the range 0.5-1. With the composition of the hybrid mixture specified, Equations S-1 to S-3, S-7, and S-8 can be used to solve for the density at the radiative-convective boundary (ρ_{rcb}). As with the pure nebular case, the mass of the atmosphere is dominated by the mass of the convective layer. Accordingly, the radius of the radiative-convective boundary must be specified to calculate captured gas masses. A fully-mixed hybrid atmosphere is distinct from the pure nebular atmosphere because it hosts a compositional boundary at the Hill radius between the hybrid mixture and the nebular-composition gas. Hence, a relationship between the conditions across the compositional boundary must be specified. Hydrostatic equilibrium and thermal steady-state requires that pressure and temperature be continuous across the compositional boundary. For ideal gases, these requirements translate to a relationship between the density of the hybrid atmosphere approaching the Hill sphere (ρ_{out}) and that of the external nebula (ρ_H):

$$\rho_{out} = \rho_H \cdot \frac{\mu_H}{\bar{\mu}} \quad (\text{Eq. S-9})$$

The radius of the radiative-convective boundary (R_{rcb}) can then be expressed by an equation analogous to Eq. S-5:

$$\frac{R_{rcb}}{R_B} = \left[\ln \left(\frac{\rho_{rcb}}{\rho_{out}} \right) + \frac{R_B}{R_H} \right]^{-1} \quad (\text{Eq. S-10})$$

Because the mass in the low density radiative layer is expected to be negligible (PISO AND YODIN, 2014), the mass of both the nebular captured gas and the outgassed inventory can be expressed by integrating the density structure across the dense adiabatic convective layer (GINZBURG *et al.*, 2016) and multiplying by the mass fraction deriving from the nebular and outgassed components, respectively:

$$M_H = x_H \cdot \left(\frac{\mu_H}{\bar{\mu}} \right) \cdot \left(\frac{5\pi^2}{4} \right) R_{rcb}^3 \rho_{rcb} \left(\frac{R_B'}{R_{rcb}} \right)^{\frac{1}{\gamma-1}} \quad (\text{Eq. S-11})$$

$$M_{CO_2} = (1 - x_H) \cdot \left(\frac{\mu_{CO_2}}{\bar{\mu}} \right) \cdot \left(\frac{5\pi^2}{4} \right) R_{rcb}^3 \rho_{rcb} \left(\frac{R_B'}{R_{rcb}} \right)^{\frac{1}{\gamma-1}} \quad (\text{Eq. S-12})$$

Energetics and Mechanism of Fluid Mixing

Mixing a stably-stratified fluid with a high-density deep outgassed layer and low-density shallow nebular component – as envisioned in e.g., (SAITO AND KURAMOTO, 2018) – into a fully-mixed structure considered in this work requires an energy source and a fluid dynamical mechanism to channel that energy into mixing. We briefly discuss these considerations in turn. Towards the end of Martian accretion ($M_p \approx M_{Mars}$) the compositional boundary in a stratified atmosphere between an outgassed layer and a nebular layer is ≈ 1 -2 planetary radii, depending on the outgassed volatile inventory. By contrast, in the fully-mixed hybrid atmospheres we calculate in Figure 1, the radius of the radiative-convective boundary (R_{rcb}), where most of the atmospheric mass resides, is ≈ 8.4 -46.5 planetary radii. Mixing therefore requires nearly as much energy as complete removal from the planetary potential well. To within a factor of about two, the energy required to uniformly mix an outgassed heavy component into a hybrid atmosphere is:

$$W_{grav} \cong \frac{GM_p M_{CO_2}}{R_p} \quad (\text{Eq. S-13})$$

with W_{grav} the work done in lifting the heavy gas into the fully-mixed state. Because the mass of the outgassed inventory is always much less than the planetary mass for terrestrial planets, and because this mixing occurs in the context of accretionary energy budgets of order GM_p^2/R_p , it is clear that the energy for mixing was present during accretion. A uniform composition hybrid atmosphere requires a fluid dynamical mechanism to channel $\approx 10^{-4}$ of the accretion energy into mixing. Although dust-free layered atmospheric models sometimes place the compositional boundary above the convective region and predict little mixing (SAITO AND KURAMOTO, 2018), dusty nebular atmospheres are more opaque and more likely to host an initial compositional boundary within the convective region. Because all gases are miscible, this picture is analogous to the problem of core erosion in the giant planets via convective entrainment, where more dramatic heavy element redistribution scenarios have been considered (STEVENSON, 1982). How much convective mixing actually takes place is difficult to predict from first principles. We suggest that the cosmochemical record (Fig. 2) can be used to empirically determine the degree of mixing on Mars.

Fractionation via Hydrodynamic Escape

The current $^{36}\text{Ar}/^{84}\text{Kr}$ ratio in the Martian atmosphere is lower than that of a hybrid mixture by a factor of ≈ 50 (Fig. 3). To illustrate the capacity of extreme-ultraviolet (EUV) powered hydrodynamic escape of a primordial volatile inventory to generate large depletions in argon with only modest isotopic fractionation, we consider a simple model in which multiple major species are present (ZAHNLE *et al.*, 1990; ZAHNLE AND KASTING, 2023). We arbitrarily define “major” species as those with mole fractions greater than 10%, and adopt a two-component ($\text{H}_2\text{-CO}_2$) model, neglecting a possible role for CO , CH_4 , N_2 , and He , which we assume would be present in minor abundances. After the crystallization of the magma ocean, H_2O would condense in the lower atmosphere (PAHLEVAN *et al.*, 2022) such that water vapor is not expected to play a role in the loss processes of interest. Two-component hydrodynamic escape can be described with an equation of energy balance:

$$\phi_1 m_1 + \phi_2 m_2 = \frac{1}{4} \eta_{eff} S_{euV} \frac{R_p}{GM_p} \quad (\text{Eq. S-14})$$

with ϕ_i [$\text{cm}^{-2} \text{s}^{-1}$] the number flux of component i out of the atmosphere, $m_1 (= 2 \text{ amu})$ and $m_2 (= 44 \text{ amu})$ the atomic mass of the two major constituents η_{eff} the efficiency factor, which is a parameter (0-1) that represents the fraction of incoming EUV energy that is channelled into mass-loss, S_{euV} [$\text{erg cm}^{-2} \text{s}^{-1}$] is the EUV flux of the young Sun at the top of the atmosphere, and the factor of 4 reflects a spherical average. η_{eff} embodies all uncertainties of the energy budget into one parameter. According to (ZAHNLE AND KASTING, 2023), S_{euV} is $133 \text{ erg cm}^{-2} \text{s}^{-1}$ at Mars’s heliocentric distance for the first few tens of millions of years of Solar System history. For these calculations, we adopt this value as a constant.

Solving for the two fluxes requires one additional constraint. Above the homopause, molecular diffusion exceeds eddy diffusion – by definition – such that the different species can partially separate via diffusion and assume different scale heights. In hydrostatic atmospheres, this separation populates the upper atmosphere in lighter species allowing for mass-fractionation accompanying non-thermal escape processes (JAKOSKY *et al.*, 2017). Such diffusive separation by mass also occurs in hydrodynamic outflows. One way to make the problem tractable is to assume an isothermal outflow, for which one can write the approximate relation (ZAHNLE AND KASTING, 2023):

$$\phi_1 \left(1 + \frac{x_2}{x_1}\right) - \phi_2 \left(1 + \frac{x_1}{x_2}\right) = \frac{g(m_2 - m_1)b_{12}}{k_B T} \quad (\text{Eq. S-15})$$

with x_1 and x_2 the mole fraction of the 1st and 2nd component, g the gravitational acceleration, b_{12} [$\text{cm}^{-1} \text{s}^{-1}$] the binary diffusion coefficient of the gas pair, k_B Boltzmann’s constant, and T the temperature of the escaping region. For concreteness, we adopt $T = 1,000 \text{ K}$ for all escape calculations. Binary diffusion coefficients measure the ease with which one gas diffuses through another. The values for binary diffusion coefficients for all gas pairs used in this work are listed in Table S-2. With Eq. S-14 and S-15, we can solve for the flux of H_2 (ϕ_1) and CO_2 (ϕ_2) as a function of the hydrodynamic escape efficiency parameter η_{eff} .

With fluxes of major species specified, the passive response of noble gases as witnesses of events can be described. For an increasingly vigorous outflow, increasingly massive gaseous species can be accelerated to space via frequent collisions with the outgoing gases. The outgoing flux (ϕ_j) of a trace species with given atomic mass (m_j) and mole fraction (x_j) can, in the isothermal approximation, be written (ZAHNLE AND KASTING, 2023):

$$\frac{\phi_j}{x_j} \left(\frac{x_1}{b_{1j}} + \frac{x_2}{b_{2j}} \right) = \frac{g(m_2 - m_j)}{k_B T} + \frac{\phi_2}{x_2} \left(\frac{x_1}{b_{12}} + \frac{x_2}{b_{2j}} \right) + \frac{\phi_1}{x_1} \left(\frac{x_1}{b_{1j}} - \frac{x_2}{b_{12}} \right) \quad (\text{Eq. S-16})$$

To calculate isotopic fractionation, an equation like Eq. S-16 is written for each of the isotopic species, keeping in mind that in some cases the binary diffusion coefficient of two gases noticeably changes upon isotopic substitution (Table S-2). The fractionation factor (α) is the ratio of the ($^{36}\text{Ar}/^{38}\text{Ar}$) of the outflowing gas relative to that of the atmosphere from which it is sourced:

$$\alpha = \frac{(\phi_{36\text{Ar}}/x_{36\text{Ar}})}{(\phi_{38\text{Ar}}/x_{38\text{Ar}})} \quad (\text{Eq. S-17})$$

With an expression for the fractionation factor (α), the evolution of the Martian atmosphere $^{36}\text{Ar}/^{38}\text{Ar}$ ratio (R_{final}) as a function of the initial ratio ($R_{initial}$) and the fraction of ^{36}Ar remaining (F) at the conclusion of the hydrodynamic episode can be related with the Rayleigh fractionation formula:

$$R_{final} = R_{initial} F^{\alpha-1} \quad (\text{Eq. S-18})$$

In the case of Kr, no mass-dependent fractionation is detectable in the Martian atmosphere (PEPIN, 1991). The hybrid mixture model requires that Mars preserve its nebular heritage by experiencing negligible mass-selective Kr escape for the duration of the hydrodynamic episode. In the context of the adopted two-component ($\text{H}_2\text{-CO}_2$) model, this leads to the requirement that the escape fluxes (ϕ_1, ϕ_2) remain below their critical values for Kr entrainment. The critical fluxes can be expressed by setting $\phi_j=0$ in Eq. S-16. The corresponding joint constraint on ϕ_1 and ϕ_2 can be used, in concert with Eq. S-14 and S-15, to define the conditions for the onset of Kr escape. Importantly, there is a range of outgoing fluxes sufficiently low as to retain Kr while sufficiently high to lose ^{36}Ar and ^{38}Ar indiscriminately enough to be consistent with the observations (Fig. 4). We propose these fluxes characterize losses from the hybrid atmosphere.

Finally, because the diffusion properties of Kr and Xe are similar, Kr retention also implies Xe retention. Hence, the Xe loss required to reproduce the Kr/Xe ratio (Fig. 3) and Xe isotopic mass-fractionation in the Martian atmosphere must be due to another process. By measurement of trapped atmospheric gases in Martian meteorites, it has recently been inferred that the isotopic evolution of Martian Xe took place over hundreds of millions of years (CASSATA *et al.*, 2022). As on the Earth, where Xe isotopic evolution apparently persisted for two gigayears (AVICE *et al.*, 2018), the Xe loss process may have involved ionization (ZAHNLE *et al.*, 2019). If so, the xenon loss may have been decoupled from the hydrodynamic loss episode of the hybrid Martian atmosphere as neutral atoms and molecules calculated here.

Supplementary Tables

Table S-1 Adopted relative elemental abundances in cosmochemical reservoirs.

Element	H chondrite ^{1,2}	EH chondrite ^{1,2}	Solar ³	Mars ^{4,5}
H	0.000459	0.001309	1E12	16.2
C	0.0001	0.000342	2.88E8	0.16
N	2.43E-6	0.00004	7.94E7	8.8E-3
Ar	1.11E-12	1.63E-11	4.17E6	1.9E-6
Kr	2.14E-13	2.50E-13	2.29E3	6.1E-8
Xe	3.82E-14	6.11E-13	2.24E2	6.8E-9

¹ H, C, N (SCHAEFER AND FEGLEY, 2017)

² Ar, Kr, Xe (SCHULTZ *et al.*, 1991; PATZER AND SCHULTZ, 2002)

³ Corrected for heavy element settling in the Sun (LODDERS, 2003)

⁴ H from a ≈ 500 m global equivalent layer (GEL) of water (DI ACHILLE AND HYNEK, 2010)

⁵ C, N, Ar, Kr, Xe from (HALLIDAY, 2013)

Table S-2 Binary diffusion coefficients for hydrodynamic escape model

Gas pair	b ($\text{cm}^{-1} \text{s}^{-1}$)	Source or scaling
$\text{H}_2\text{-CO}_2$	$4.1 \times 10^{19} (T/1000)^{0.75}$	Zahnle and Kasting (1986)
$^{36}\text{Ar-H}_2$	$5.0 \times 10^{19} (T/1000)^{0.75}$	Zahnle and Kasting (1986)
$^{38}\text{Ar-H}_2$	$5.0 \times 10^{19} (T/1000)^{0.75}$	Scaled from $^{36}\text{Ar-H}_2$
$^{84}\text{Kr-H}_2$	$4.4 \times 10^{19} (T/1000)^{0.76}$	Zahnle and Kasting (1986)
$^{36}\text{Ar-CO}_2$	$1 \times 10^{19} (T/1000)^{0.75}$	Zahnle and Kasting (2023)
$^{38}\text{Ar-CO}_2$	$0.985 \times 10^{19} (T/1000)^{0.75}$	Scaled from $^{36}\text{Ar-CO}_2$
$^{84}\text{Kr-CO}_2$	$0.78 \times 10^{19} (T/1000)^{0.75}$	Scaled from $^{36}\text{Ar-CO}_2$ ¹

¹ Scaling across elements requires kinetic diameters.: Ar: 340 pm; Kr: 360 pm; CO₂: 330 pm

Supplementary Information References

- Avice, G., Marty, B., Burgess, R., Hofmann, A., Philippot, P., Zahnle, K., Zakharov, D. (2018) Evolution of atmospheric xenon and other noble gases inferred from Archean to Paleoproterozoic rocks. *Geochimica et Cosmochimica Acta* 232, 82-100.
- Bell, K., Lin, D. (1994) Using FU Orionis outbursts to constrain self-regulated protostellar disk models. *Astrophysical Journal, Part 1 (ISSN 0004-637X)*, vol. 427, no. 2, p. 987-1004 427, 987-1004.
- Cassata, W.S., Zahnle, K.J., Samperton, K.M., Stephenson, P.C., Wimpenny, J. (2022) Xenon isotope constraints on ancient Martian atmospheric escape. *Earth and Planetary Science Letters* 580, 117349.
- Chambers, J. (2017) Steamworlds: atmospheric structure and critical mass of planets accreting icy pebbles. *The Astrophysical Journal* 849, 30.
- Di Achille, G., Hynek, B.M. (2010) Ancient ocean on Mars supported by global distribution of deltas and valleys. *Nature Geoscience* 3, 459.
- Ginzburg, S., Schlichting, H.E., Sari, R.e. (2016) Super-Earth Atmospheres: Self-consistent Gas Accretion and Retention. *The Astrophysical Journal* 825, 29.
- Halliday, A.N. (2013) The origins of volatiles in the terrestrial planets. *Geochimica et Cosmochimica Acta* 105, 146-171.
- Hayashi, C. (1981) Structure of the solar nebula, growth and decay of magnetic fields and effects of magnetic and turbulent viscosities on the nebula. *Progress of Theoretical Physics Supplement* 70, 35-53.
- Hayashi, C., Nakazawa, K., Mizuno, H. (1979) Earth's melting due to the blanketing effect of the primordial dense atmosphere. *Earth and Planetary Science Letters* 43, 22-28.
- Ikoma, M., Genda, H. (2006) Constraints on the Mass of a Habitable Planet with Water of Nebular Origin. *The Astrophysical Journal* 648, 696.
- Jakosky, B.M., Sliwski, M., Benna, M., Mahaffy, P., Elrod, M., Yelle, R., Stone, S., Alsaeed, N. (2017) Mars' atmospheric history derived from upper-atmosphere measurements of $^{38}\text{Ar}/^{36}\text{Ar}$. *Science* 355, 1408-1410.
- Kittel, C., Kroemer, H. (1998) Thermal physics. American Association of Physics Teachers.
- Lodders, K. (2003) Solar system abundances and condensation temperatures of the elements. *The Astrophysical Journal* 591, 1220.
- Pahlevan, K., Schaefer, L., Elkins-Tanton, L.T., Desch, S.J., Buseck, P.R. (2022) A primordial atmospheric origin of hydrospheric deuterium enrichment on Mars. *Earth and Planetary Science Letters* 595, 117772.
- Patzer, A., Schultz, L. (2002) Noble gases in enstatite chondrites II: The trapped component. *Meteoritics & Planetary Science* 37, 601-612.
- Pepin, R.O. (1991) On the origin and early evolution of terrestrial planet atmospheres and meteoritic volatiles. *Icarus* 92, 2-79.
- Piso, A.-M.A., Youdin, A.N. (2014) On the Minimum Core Mass for Giant Planet Formation at Wide Separations. *The Astrophysical Journal* 786, 21.
- Saito, H., Kuramoto, K. (2018) Formation of a hybrid-type proto-atmosphere on Mars accreting in the solar nebula. *Monthly Notices of the Royal Astronomical Society* 475, 1274-1287.
- Schaefer, L., Fegley, B. (2017) Redox States of Initial Atmospheres Outgassed on Rocky Planets and Planetesimals. *The Astrophysical Journal* 843, 120.
- Schultz, L., Weber, H., Begemann, F. (1991) Noble gases in H-chondrites and potential differences between Antarctic and non-Antarctic meteorites. *Geochimica et Cosmochimica Acta* 55, 59-66.
- Stevenson, D.J. (1982) Formation of the giant planets. *Planetary and Space Science* 30, 755-764.
- Zahnle, K., Kasting, J.F., Pollack, J.B. (1990) Mass fractionation of noble gases in diffusion-limited hydrodynamic hydrogen escape. *Icarus* 84, 502-527.
- Zahnle, K.J., Gacesa, M., Catling, D.C. (2019) Strange messenger: A new history of hydrogen on Earth, as told by Xenon. *Geochimica et Cosmochimica Acta* 244, 56-85.
- Zahnle, K.J., Kasting, J.F. (2023) Elemental and isotopic fractionation as fossils of water escape from Venus. *Geochimica et Cosmochimica Acta* 361, 228-244.